


DNMT3a contributes to the development and maintenance of bone cancer pain by silencing Kv1.2 expression in spinal cord dorsal horn

Xue-Rong Miao*^{1,2}, Long-Chang Fan^{2,3}, Shaogen Wu²,
Qing-Xiang Mao², Zhen Li², Brianna M Lutz², Jitian Xu^{2,4},
Zhi-Jie Lu¹ and Yuan-Xiang Tao^{2,4,5,6}

Molecular Pain
Volume 13: 1–14
© The Author(s) 2017
Reprints and permissions:
sagepub.com/journalsPermissions.nav
DOI: 10.1177/1744806917740681
journals.sagepub.com/home/mpx


Abstract

Metastatic bone tumor-induced changes in gene transcription and translation in pain-related regions of the nervous system may participate in the development and maintenance of bone cancer pain. Epigenetic modifications including DNA methylation regulate gene transcription. Here, we report that intrathecal injection of decitabine, a DNA methyltransferase (DNMT) inhibitor, dose dependently attenuated the development and maintenance of bone cancer pain induced by injecting prostate cancer cells into the tibia. The level of the *de novo* DNMT3a, but not DNMT3b, time dependently increased in the ipsilateral L4/5 dorsal horn (not L4/5 dorsal root ganglion) after prostate cancer cells injection. Blocking this increase through microinjection of recombinant adeno-associated virus 5 (AAV5) expressing *Dnmt3a* shRNA into dorsal horn rescued prostate cancer cells-induced downregulation of dorsal horn Kv1.2 expression and impaired prostate cancer cells-induced pain hypersensitivity. In turn, mimicking this increase through microinjection of AAV5 expressing full-length *Dnmt3a* into dorsal horn reduced dorsal horn Kv1.2 expression and produced pain hypersensitivity in the absence of prostate cancer cells injection. Administration of neither decitabine nor virus affected locomotor function and acute responses to mechanical, thermal, or cold stimuli. Given that *Dnmt3a* mRNA is co-expressed with *Kcna2* mRNA (encoding Kv1.2) in individual dorsal horn neurons, our findings suggest that increased dorsal horn DNMT3a contributes to bone cancer pain through silencing dorsal horn Kv1.2 expression. DNMT3a may represent a potential new target for cancer pain management.

Keywords

DNMT3a, Kv1.2, dorsal horn, cancer pain

Date received: 1 September 2017; revised: 28 September 2017; accepted: 3 October 2017

¹Department of Anesthesiology and Intensive Care, Third Affiliated Hospital of Second Military Medical University, Shanghai, China

²Department of Anesthesiology, New Jersey Medical School, Rutgers, The State University of New Jersey, Newark, NJ, USA

³Department of Anesthesiology, Tongji Hospital, Tongji Medical College, Huazhong University of Science and Technology, Wuhan, China

⁴Neuroscience Research Institute, College of Basic Medicine, Zhengzhou University, Zhengzhou, Henan, China

⁵Department of Cell Biology & Molecular Medicine, Rutgers New Jersey Medical School, The State University of New Jersey, Newark, NJ, USA

⁶Department of Pharmacology, Physiology & Neuroscience, Rutgers New Jersey Medical School, The State University of New Jersey, Newark, NJ, USA

Xue-Rong Miao and Long-Chang Fan equally contributed to this work.

Corresponding authors:

Yuan-Xiang Tao, Department of Anesthesiology, New Jersey Medical School, Rutgers, The State University of New Jersey, 185 S. Orange Ave., MSB, E-661, Newark, NJ 07103, USA.

Email: yuanxiang.tao@njms.rutgers.edu

Xue-Rong Miao, Department of Anesthesiology and Intensive Care, Third Affiliated Hospital of Second Military Medical University, 225 Changhai Road, No.2 Building, 3rd Floor, Shanghai 200438, China.

Email: miaoxr@smmu.edu.cn



Introduction

Cancer-induced bone pain, one of the most common clinical symptoms, is present in around one third of patients with bone metastasis that is caused predominantly by cancer of the prostate, breast, and lung.¹ Bone cancer pain is intractable and persistent.^{2,3} Health care expenses and lost productivity account for over 600 billion dollars in spending each year due to chronic pain including cancer pain.⁴ Although multiple drugs like antidepressants (e.g., amitriptyline and duloxetine), anti-convulsants (e.g., gabapentin and carbamazepine), and opioids (e.g., morphine) have been used for the treatment of bone cancer pain, the majority of patients exhibit unsatisfactory pain control and/or require higher doses of drugs and repeated and long-term administration of the drugs (e.g., opioids). The consequence of these drug regimens leads to severe side effects including nausea, dizziness, cardiac arrhythmia, cognitive changes, constipation, respiratory depression, opioid analgesic tolerance and hyperalgesia, and addiction, which significantly limit the use of these anti-nociceptive drugs in cancer patients. Understanding how bone cancer pain develops and persists may be essential for improving patient care. Peripheral nerve ending and tissue damages in the bone caused by cancer invasion lead to unique changes in gene transcription and translation of receptors, ion channels, and enzymes in the dorsal root ganglion (DRG), spinal cord, and brain regions.^{5–7} We previously demonstrated that spinal cord dorsal horn protein translation was required for the development and maintenance of bone cancer pain.⁸ Whether the changes in gene transcription participate in the bone cancer pain genesis is still unknown.

Epigenetic modifications including DNA methylation predominantly regulate gene transcription.^{9,10} In mammalian cells, DNA methylation occurs mostly on the fifth carbon of cytosine residues situated adjacent to a guanine residue (CpG site). CpG islands that contain clusters of CpGs are often located near the promoter and 5'-untranslated region of a gene. DNA methylation is catalyzed by DNA methyltransferases (DNMTs), including DNMT1, DNMT3a, and DNMT3b. DNMT1 is responsible for the maintenances of methylation patterns, whereas DNMT3a and DNMT3b are responsible for *de novo* methylation and are generally associated with gene silencing.^{11–14} Recent evidence showed that DNMT3a and its triggered DNA methylation contribute to neuropathic pain through the silencing of opioid receptors and potassium channel genes in the DRG.^{15–18} However, whether and how DNMT3a is involved in bone cancer pain is unclear.

In the present study, we hypothesized that DNMT3a might participate in the development and maintenance of bone cancer-induced pain by silencing gene expression in pain-related regions. To this end, we first observed the

protein expression of DNMT3a in two pain-related regions, DRG and spinal dorsal horn, after prostate cancer cell (PCC) intra-tibia injection. We then investigated the effect of pharmacologic inhibition or knock-down of dorsal horn DNMT3a on the development and maintenance of PCC-induced bone cancer pain. Finally, we defined whether PCC injection altered the gene expression of potassium channels, opioid receptors, and glutamic acid decarboxylases in the spinal cord and whether these altered genes were regulated by spinal cord DNMT3a.

Materials and methods

Animals

All experiments were performed in accordance with the NIH Guidelines for the Care and Use of Laboratory Animals and the ethical guidelines of the US National Institutes of Health and the International Association for the Study of Pain and were approved by the Institutional Animal Care and Use Committee at Rutgers New Jersey Medical School (Newark, NJ). Adult male Copenhagen rats weighing 200–225 g were housed under a 12-h light/dark cycle in a pathogen-free area with *ad libitum* access to water and food. Animals were trained for one to two days before behavioral testing was performed. The experimenters were blind to drug treatment condition during the behavioral testing.

Cell lines, drugs, and virus

The AT-3.1 PCC line was obtained from American Type Culture Collection (ATCC, Manassas, VA). The DNMT inhibitor 5-aza-2'-deoxycytidine (decitabine) was purchased from Sigma (St. Louis, MO). Decitabine was dissolved in saline. Recombinant adeno-associated virus 5 (AAV5) expressing *Dnmt3a* shRNA (AAV5-*Dnmt3a* shRNA), enhanced green fluorescent protein (AAV5-GFP), or full-length *Dnmt3a* (AAV5-*Dnmt3a*) was prepared as described previously.^{15,17} Virus was dissolved in phosphate-buffered saline. All drug/virus dosages used were based on data from previous studies^{15,17–21} and our pilot work.

PCC preparation

The PCC was grown in RPMI 1640 medium (Sigma) that contained L-glutamine and was supplemented with 250 nM dexamethasone and 10% fetal bovine serum. Cells were maintained in T-75 plastic flasks (Corning Glass) and cultured in a humidified incubator with 5% CO₂. For passage, cells were detached by rinsing gently with calcium- and magnesium-free Hanks' balanced salt solution (HBSS) and a trypsin-EDTA solution.

The detached cells were collected by centrifugation of 10 mL of medium for 3 min at 1200 r/min. The resulting pellet was washed twice with 10 mL of calcium- and magnesium-free HBSS. The final pellet was resuspended in 1 mL of HBSS and cells were counted using a hemocytometer and trypan blue solution. Cells were diluted to the final concentration of 4.5×10^5 cells/15 μ L HBSS and kept on ice for injection.

Intrathecal catheter implantation

Rats were fully anesthetized with 2% isoflurane, and a 1-cm midline incision was made from the back. Then a PE-10 polyethylene catheter was implanted into the subarachnoid space between the L4 and L5 vertebrae to reach the lumbar enlargement of the spinal cord at a depth of 2–2.5 cm as described previously.^{22–25} The outer part of the catheter was tunneled subcutaneously to exit in the dorsal neck region, where it was secured to the superficial musculature and skin. Five to seven days after catheter implantation, rats without any locomotor deficits were chosen for intrathecal (i.th.) administration. The drugs or the virus were administered intrathecally in a 10- μ L volume followed by 12 μ L of saline for flushing.

Intraspinal cord microinjection

Spinal cord microinjection was carried out as described previously.²⁶ Briefly, after the animals were anesthetized, unilateral laminectomy of T12 vertebra was carried out and the spinal cord exposed. The rats were placed in the stereotaxic frame and the vertebral column immobilized. The glass micropipette was positioned 200 μ m lateral from the posterior median sulcus and 200 μ m below the dorsal surface of the spinal cord at the level of L5 spinal cord. Under an inverted microscope, viral solution (2 μ L, 4×10^{12}) was injected at a rate of 100 nL/min with the micropipette connected to a Hamilton syringe. The pipette was removed 10 min after injection. Two injection sites within a 1-mm interval along the posterior median sulcus were carried out. No impairment of locomotor function after microinjection was observed.

PCC-induced bone cancer pain model

PCC-induced bone cancer pain model was prepared as described in our previous study.^{8,27} Briefly, five to seven days after i.th. catheter implantation, rats were anesthetized with 2% isoflurane. The right leg was shaved and the skin was disinfected with 70% (v/v) ethanol and a 1-cm incision was made in the skin over the upper medial half of the tibia. The tibia was carefully exposed with minimal damage to the muscle. The bone was pierced with a 23-gauge needle 5 mm below the knee joint

medial to the medullary canal. A 50- μ L Hamilton syringe was used to inject 15 μ L of PCC or HBSS into the cavity. After injection, the syringe was kept in place for 2 min and was then slowly pulled out. The bone hole was sealed with bone wax (Ethicon, Somerville, NJ), and the skin was sutured with 4-0 silk threads.

Behavioral testing

Paw withdrawal latency to noxious heat stimulation was measured as described.^{21,28–30} Briefly, each animal was placed in a Plexiglas chamber on an elevated glass plate. Radiant heat from a Model336 Analgesia Meter (IITC Life Science Instruments, Woodland Hills, CA) was applied to the plantar surface of each hind paw. When the animal lifted its foot, the light beam was turned off. The length of time between the start of the light beam and the foot lift was defined as the paw withdrawal latency. Each trial was repeated five times at 5-min intervals for each paw. A cut-off time of 20 s was imposed to prevent tissue damage.

Paw withdrawal threshold to mechanical stimulation was measured in the same manner as before.^{21,28–30} In brief, each animal was placed in a Plexiglas chamber on an elevated mesh screen. Von Frey filaments in log increments of force (0.69, 1.20, 2.04, 3.63, 5.50, 8.51, 15.14, and 26 g) were applied to the plantar surface of the left and right hind paws. The 3.63-g stimulus was used first. If a positive response occurred, the next smaller von Frey hair was used, and if a negative response was observed, the next higher von Frey hair was used. The test was ended when: (1) a negative response was obtained with the 26-g hair and (2) three stimulations were applied after the first positive response. The pattern of positive and negative paw withdrawal responses to the von Frey filament stimulation was converted to a 50% threshold value using the formula provided by Dixon.³¹

Paw withdrawal latency to cold stimulation was carried out as described.^{21,28–30} Each animal was placed in a Plexiglas chamber on a cold aluminum plate, which was set at 0°C. The temperature of the plate was monitored continuously by a thermometer. The length of time between the placement of the hind paw on the plate and a flinching of the paw was defined as the paw withdrawal latency. Each trial was repeated three times at 10-min intervals for the paw on the ipsilateral side. A cut-off time of 60 s was used to avoid tissue damage.

Locomotor functions were examined as described.^{19,20} In Brief, three reflexes were performed: (1) Placing reflex: The rat was held with the hind limbs slightly lower than the forelimbs, and the dorsal surfaces of the hind paws were brought into contact with the edge of a table. The experimenter recorded whether the hind paws were placed on the table surface reflexively; (2) Grasping reflex: The rat was placed on a wire grid and the

experimenter recorded whether the hind paws grasped the wire on contact; and (3) righting reflex: The rat was placed on its back on a flat surface and the experimenter noted whether it immediately assumed the normal upright position. Scores for placing, grasping, and righting reflexes were based on counts of each normal reflex exhibited in five trials.

Western blot analysis

The ipsilateral and contralateral L4/5 dorsal horns and L4/5 DRG were collected after behavioral testing or at different time points after PCC injection. The tissues were homogenized in homogenization buffer (10 mM Tris-HCl [pH 7.4], 5 mM NaF, 1 mM sodium orthovanadate, 320 mM sucrose, 1 mM EDTA, 1 mM EGTA, .1 mM phenylmethylsulfonyl fluoride, 1 M leupeptin, and 2 mM pepstatin A). After centrifugation at $1000 \times g$ for 20 min at 4°C, the supernatant was collected for cytosolic proteins and the pellet for nuclear proteins. The samples were heated for 5 min at 95°C and then loaded onto 4% stacking and 10% separating SDS-polyacrylamide gels. The proteins were electrophoretically transferred onto nitrocellulose membrane. The blotting membranes were blocked with 3% nonfat dry milk for 1 h and incubated overnight at 4°C with the following primary antibodies: mouse anti-Kv1.2 (1:200, Neuromab), rabbit anti- β actin (1: 2,000, Bioss), rabbit anti-GAPDH (1:1,000, Santa Cruz), rabbit anti-DNMT3a (1:500; Cell Signaling), goat anti-DNMT3b (1:500; Santa Cruz), and rabbit anti-histone H3 (1:1,000, Cell Signaling). The proteins were detected using anti-rabbit or anti-mouse secondary antibody and visualized with chemiluminescence reagents provided with the ECL kit (Amersham Pharmacia Biotech, Piscataway, NJ) and exposure to film. The intensity of blots was quantified with densitometry. The blot density from naïve rats (0 days) or the AAV5-GFP plus HBSS-treated groups was set as 100%.

RNA extraction and quantitative real-time reverse transcription polymerase chain reaction

Quantitative real-time reverse transcription polymerase chain reaction (RT-PCR) analysis was carried out as described.^{19,20} Briefly, total RNA from dorsal horn was extracted by the Trizol method (Invitrogen, Carlsbad, CA), treated with DNase I (New England Biolabs, Ipswich, MA), and reverse-transcribed using the ThermoScript reverse transcriptase (Invitrogen), oligo (dT) primers or specific RT-primers (Table 1). RT products were amplified by real-time PCR using the primers listed in the Table 1. Glyceraldehyde-3-phosphate dehydrogenase (*Gapdh*) was used as an internal control for normalization. Each sample was run in triplicate in a

Table 1. All primers used.

Names	Sequences (5'-3')
Kcna1-RT	5'-AAAGTATCTACAGAGTGGGACA-3'
Kcna1-F	5'-GACTTCACGGGCACCATTACAC-3'
Kcna1-R	5'-TCAAAAAGAGAACCAGATGATACAC-3'
Kcna2-RT	5'-GGGTGACTCTCATCTTTGGA-3'
Kcna2-F	5'-CCCATCTGCAAGGGCAACGT-3'
Kcna2-R	5'-CACAGCCTCCTTTGGCTGGC-3'
Kcna4-RT	5'-ACGGCACAATCCCAACAAT-3'
Kcna4-F	5'-CCCATACCTACCTTCTAATTTGC-3'
Kcna4-R	5'-TGTTTTTATCTGTCTCGCTGTCA-3'
Oprd1-F	5'-GGGTCTTGGCTTCAGGTGTT-3'
Oprd1-R	5'-ACGGTGATGATGAGAATGGG-3'
Oprm1-F	5'-TTCCTGGTCATGTATGTGATTGTA-3'
Oprm1-R	5'-GGGCAGTGTACTGGTCGCTAA-3'
Oprk1-F	5'-TTTGTGGTGGGCTTAGTGGG-3'
Oprk1-R	5'-CTCTGGAAGGGCATAGTGGT-3'
Gad1-F	5'-TAAGAACGGGGAGGAGCAAAC-3'
Gad1-R	5'-AGACTCGGGGTGGTCAGACAG-3'
Gad2-F	5'-GACGCACTGCCAAACAACCTCT-3'
Gad2-R	5'-CAACCAATCTGCTGCTAATCC-3'
Dnmt3a-F	5'-GTGGTTCGGAGATGGCAAAT-3'
Dnmt3a-R	5'-TGGAGGACTTCGTAGATGGCT-3'
Gapdh-RT	5'-TCCTGTTGTTATGGGGTCTG-3'
Gapdh-F	5'-TCGGTGTGAACGGATTGGC-3'
Gapdh-R	5'-CCTTCAGGTGAGCCCCAGC-3'

RT: reverse transcription; F: forward; R: reverse.

20 μ L reaction with 250 nM forward and reverse primers, 10 μ L of Advanced Universal SYBR Green Supermix (Bio-Rad Laboratories, Hercules, CA), and 20 ng of cDNA. Reactions were performed in a Bio-Rad CFX96 real-time PCR system. Ratios of ipsilateral-side mRNA levels to contralateral-side mRNA levels were calculated using the $\Delta\Delta C_t$ method ($2^{-\Delta\Delta C_t}$) at a threshold of 0.02. All data were normalized to *Gapdh*.

For single-cell RT-PCR, freshly dissociated rat dorsal horn neurons were first prepared as described previously.^{17,22,28,32} Briefly, 4 h after plating, the neuron was randomly harvested under an inverted microscope fit with a micromanipulator and microinjector and placed in a PCR tube with 5–10 μ L of cell lysis buffer (Signosis, Sunnyvale, CA). After centrifugation, the supernatants were collected and divided into three PCR tubes for *Kcna2*, *Dnmt3a*, and *Gapdh* genes. The remaining real-time RT-PCR procedure was carried out according to the manufacturer's instructions with the single-cell real-time RT-PCR assay kit (Signosis). All primers used are listed in Table 1. After amplification, PCR products were separated on a 2.0% agarose gel containing

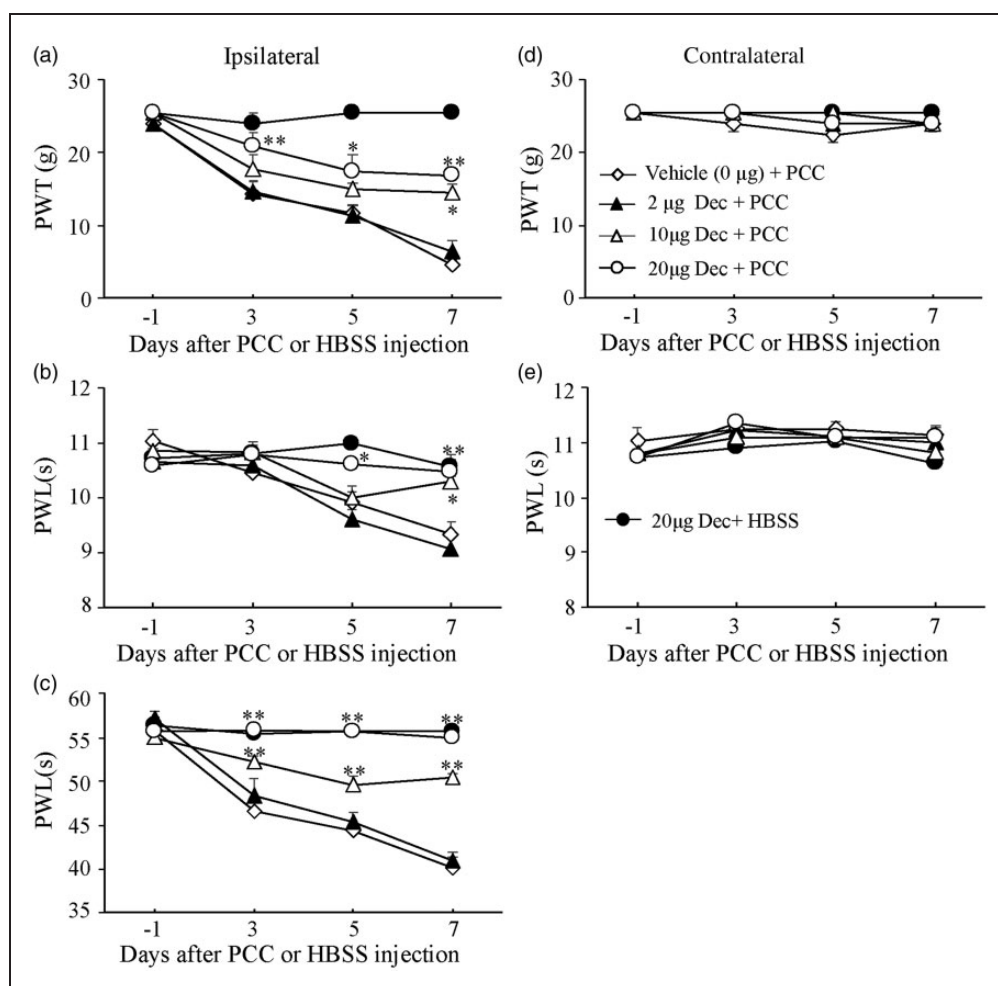


Figure 1. Effect of intrathecal administration of decitabine (Dec) on the development of mechanical allodynia, thermal hyperalgesia, and cold allodynia induced by injecting prostate cancer cells (PCC) into the tibia. Decitabine given once daily for seven days dose dependently blocked PCC-induced decreases in paw withdrawal threshold (PWT) to mechanical stimulation (a) and paw withdrawal latency (PWL) to thermal (b) or cold (c) stimulation on the ipsilateral side. Decitabine at 20 µg alone did not affect basal responses to mechanical, thermal, or cold stimuli on the ipsilateral side in rats injected with Hank's balance salt solution (HBSS, (a) to (c)). Decitabine at the doses used did not affect basal responses to mechanical (d) and thermal (e) stimuli on the contralateral side. $n = 5/\text{group}$. Two-way ANOVA followed by post hoc Tukey's test. $*P < 0.05$, $**P < 0.01$ versus the vehicle plus PCC group at the corresponding time points.

0.025% ethidium bromide; bands were visualized using ChemiDoc™ XRS + Imaging Systems (Bio-Rad Laboratories).

Statistical analysis

The results from the behavioral tests, RT-PCR, and Western blotting were analyzed with a one-way or two-way analysis of variance. Data are presented as means \pm SEM. When analysis of variance showed significant difference, pairwise comparisons between means were tested by the post hoc Tukey's method. The statistical software package SigmaPlot 12.5 (Systat Software Inc., USA) was used to perform all statistical analyses. All probability values were two tailed and significance was set at $P < 0.05$.

Results

Effect of i.th. DNMT inhibitors on the development of PCC-induced bone cancer Pain

To demonstrate the role of spinal DNMTs in the development of bone cancer pain, we carried out the PCC-induced bone cancer pain model as described in our previous study.⁸ Decitabine, a cytosine analog that inhibits DNMTs and results in DNA hypomethylation, was administered i.th. once daily for seven days after injection of HBSS or PCC. I.th. administration of 20 µg decitabine ($n = 5$) significantly attenuated PCC-induced mechanical allodynia, thermal hyperalgesia, and cold allodynia on the ipsilateral side during the development period (Figure 1(a) to (c)). These effects were dose dependent (Figure 1(a) to (c)). On day 7

Table 2. Locomotor test.

Treated groups	Placing	Grasping	Righting
20 μ g decitabine + HBSS	5(0)	5(0)	5(0)
Vehicle + PCC	5(0)	5(0)	5(0)
2 μ g decitabine + PCC	5(0)	5(0)	5(0)
10 μ g decitabine + PCC	5(0)	5(0)	5(0)
20 μ g decitabine + PCC	5(0)	5(0)	5(0)
AAV5-GFP + PCC	5(0)	5(0)	5(0)
AAV5-scrambled shRNA + PCC	5(0)	5(0)	5(0)
AAV5- <i>Dnmt3a</i> shRNA + PCC	5(0)	5(0)	5(0)
AAV5- <i>Dnmt3a</i>	5(0)	5(0)	5(0)
AAV5-GFP	5(0)	5(0)	5(0)

N=4-8/group, five trials, mean (SEM). GFP: green fluorescent protein; HBSS: Hanks' balanced salt solution; PCC: prostate cancer cells.

after PCC injection, the 20- μ g dose of decitabine increased paw withdrawal threshold to mechanical stimulation by 3.67 fold ($P < 0.01$), the 10- μ g dose by 3.16 fold ($n = 5$, $P < 0.05$), and the 2- μ g dose by 1.41 fold ($n = 5$, $P > 0.05$) compared to the corresponding PCC-injected group treated with the vehicle (saline, $n = 5$, Figure 1(a)). Similarly, on day 7 after PCC injection, the 20- μ g dose of decitabine increased paw withdrawal latencies to thermal and cold stimuli by 1.12 fold ($n = 5$, $P < 0.01$) and 1.3 fold ($n = 5$, $P < 0.01$), respectively, the 10- μ g dose by 1.1 fold ($n = 5$, $P < 0.05$) and 1.25 fold ($n = 5$, $P < 0.01$), respectively, and the 2- μ g dose by 0.97 fold ($n = 5$, $P > 0.05$) and 1.02 fold ($n = 5$, $P > 0.05$), respectively, compared to the corresponding PCC-injected group treated with the vehicle ($n = 5$, Figure 1(b) and (c)). Neither decitabine at the doses used nor vehicle markedly changed basal paw withdrawal responses to mechanical and thermal stimuli on the contralateral side during the observation period (Figure 1(d) and (e)). As expected, the 20- μ g dose of decitabine alone did not affect basal paw withdrawal responses to mechanical, thermal, or cold stimuli in the HBSS-treated rats ($n = 5$, Figure 1(a) to (e)). In addition, i.th. decitabine at the doses used did not alter locomotor function as demonstrated by no significant differences in placing, grasping, and righting reflexes among the treated groups (Table 2).

Effect of i.th. DNMT inhibitors on the maintenance of PCC-induced bone cancer Pain

To further investigate the role of spinal DNMTs in the maintenance of bone cancer pain, we administered decitabine or vehicle i.th. once daily for five days starting at day 7 post-PCC injection. Decitabine at 20 μ g ($n = 5$) significantly alleviated PCC-induced mechanical

allodynia, thermal hyperalgesia, and cold allodynia on the ipsilateral side during the maintenance period (Figure 2(a) to (c)). The effects of decitabine were dose dependent (Figure 2(a) to (c)). On day 12 after PCC injection, the 20- μ g dose of decitabine increased paw withdrawal threshold to mechanical stimulation by 4.52 fold ($P < 0.01$) and the 10- μ g dose by 3.27 fold ($n = 5$, $P < 0.01$) compared to the corresponding PCC-injected group treated with the vehicle (saline, $n = 5$, Figure 2(a)). The 2- μ g dose of decitabine had no effect on PCC-induced reduction in paw withdrawal thresholds (Figure 1(a), $n = 5$, $P > 0.05$). Likewise, on day 12 after PCC injection, the 20- μ g dose of decitabine increased paw withdrawal latencies to thermal and cold stimuli by 1.14 fold ($n = 5$, $P < 0.01$) and 1.44 fold ($n = 5$, $P < 0.01$), respectively, the 10- μ g dose by 1.08 fold ($n = 5$, $P < 0.01$) and 1.31 fold ($n = 5$, $P < 0.01$), respectively, and the 2- μ g dose by 1.0 fold ($n = 5$, $P > 0.05$) and 1.07 fold ($n = 5$, $P > 0.05$), respectively, compared to the corresponding PCC-injected group treated with the vehicle ($n = 5$, Figure 2(b) and (c)). As expected, decitabine did not change basal paw withdrawal responses to mechanical or thermal stimulation applied to the contralateral hind paw during the maintenance period (Figure 2(d) and (e)). Decitabine alone did not affect basal paw withdrawal responses to mechanical and thermal stimuli on bilateral sides of the HBSS-treated rats during the maintenance period ($n = 5$, Figure 2(a) to (e)).

Time-dependent increase of DNMT3a in spinal dorsal horn after PCC injection

The behavioral studies described above suggest that the activity of DNMTs may be changed and that this change may be required for the development and maintenance of bone cancer pain. To test our conclusion, we next examined the expression of two *de novo* DNMTs, DNMT3a and DNMT3b, in two pain-related regions, DRG and spinal dorsal horn. The tissues from the ipsilateral and contralateral L4/5 DRG and spinal dorsal horn at 0, 3, 5, 7, and 12 days after PCC or HBSS injection were harvested. The amounts of DNMT3a protein markedly and time dependently increased in the ipsilateral (but not contralateral) L4/5 dorsal horn after PCC injection (Figure 3(a) and (b)). This increase appeared at day 3, reached a peak at day 7, and persisted for at least 12 days post-PCC injection (Figure 3(a)). Interestingly, the expression of another *de novo* methyltransferase DNMT3b protein did not change in both ipsilateral and contralateral L4/5 dorsal horn during the observation period (Figure 3(a) and (b)). As expected, HBSS injection did not alter the basal expression of both DNMT3a and DNMT3b proteins in the ipsilateral L4/5 dorsal horn (Figure 3(c)). Unexpectedly, the levels of DNMT3a and DNMT3b proteins were not

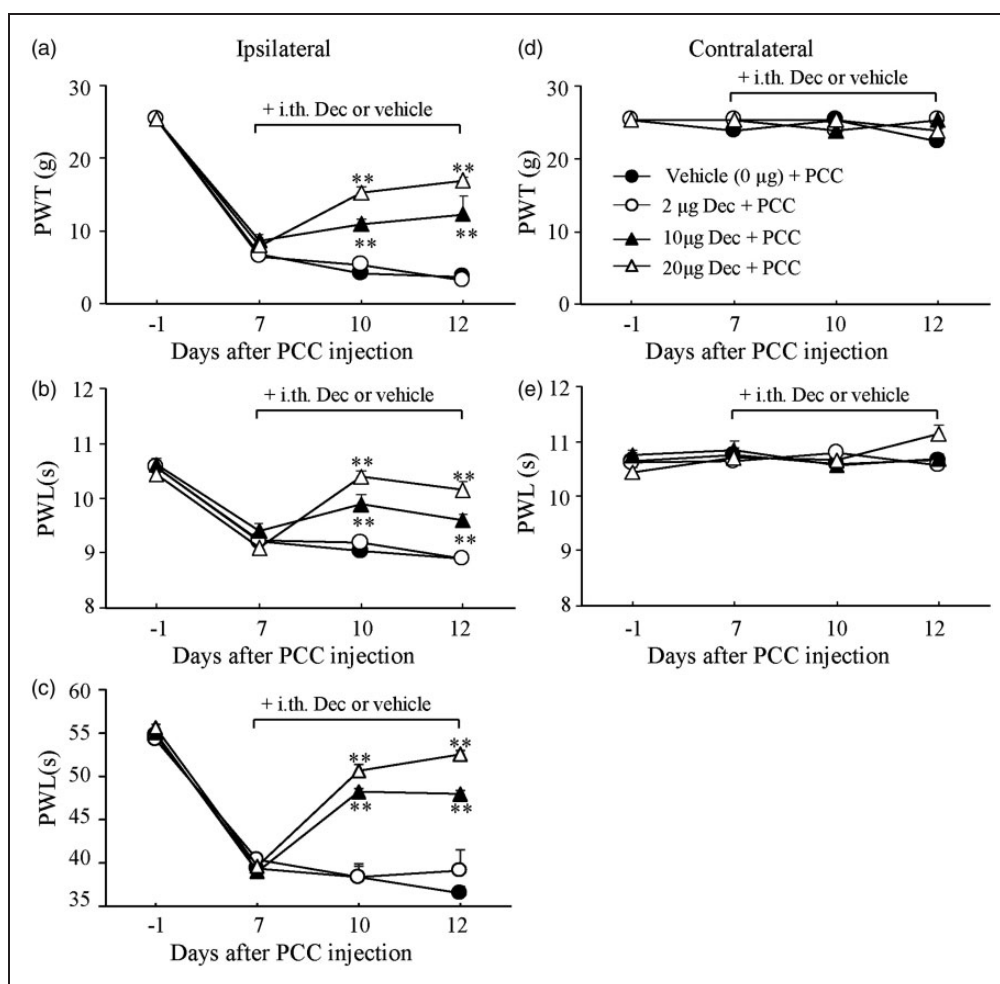


Figure 2. Effect of intrathecal administration of decitabine on the maintenance of mechanical allodynia, thermal hyperalgesia, and cold allodynia induced by injecting prostate cancer cells (PCC) into the tibia. Decitabine given once daily for five days starting at day 7 post-PCC injection dose dependently attenuated PCC-induced decreases in paw withdrawal threshold (PWT) to mechanical stimulation (a) and paw withdrawal latency (PWL) to thermal (b) or cold (c) stimulation on the ipsilateral side. Post-treatment with decitabine at the doses used did not affect basal responses to mechanical (d) and thermal (e) stimuli on the contralateral side of PCC rats. $n = 5/\text{group}$. Two-way ANOVA followed by post hoc Tukey's test. $***P < 0.01$ versus the vehicle plus PCC group at the corresponding time points.

significantly changed in the ipsilateral L4/5 DRG following PCC injection (Figure 3(d)).

Effect of dorsal horn DNMT3a knockdown on the development of PCC-induced cancer pain

Is the increased dorsal horn DNMT3a involved in the development of PCC-induced bone cancer pain? To answer this question, we microinjected AAV5-*Dnmt3a* shRNA into unilateral L4/5 dorsal horn. AAV5-scrambled shRNA or AAV5-GFP was used as a control. Specificity and selectivity of *Dnmt3a* shRNA have been verified in our previous studies.^{15,17} Consistently, microinjection of AAV5-*Dnmt3a* shRNA ($n = 5$), but not AAV5-scrambled shRNA ($n = 5$) and AAV5-GFP ($n = 5$), 30 days before PCC injection significantly

blocked the PCC-induced increase of DNMT3a protein without affecting the basal expression of DNMT3b in dorsal horn on day 7 post-PCC injection (Figure 4(a) and (b)). This microinjection attenuated PCC-induced mechanical allodynia, thermal hyperalgesia, and cold allodynia on the ipsilateral side from day 5 to 7 post-PCC injection (Figure 4(c) to (e)). On day 7 after PCC injection, rats pre-treated with AAV5-*Dnmt3a* shRNA displayed increases in paw withdrawal threshold to mechanical stimulation by 4.04 fold ($P < 0.01$) and in paw withdrawal latencies to thermal and cold stimuli by 1.09 fold ($P < 0.01$) and 1.35 fold ($P < 0.01$), respectively, compared to the corresponding PCC-injected rats treated with the AAV5-GFP (Figure 4(c) to (e)). No changes were seen in basal mechanical, thermal, or cold responses on the contralateral sides of PCC-injected

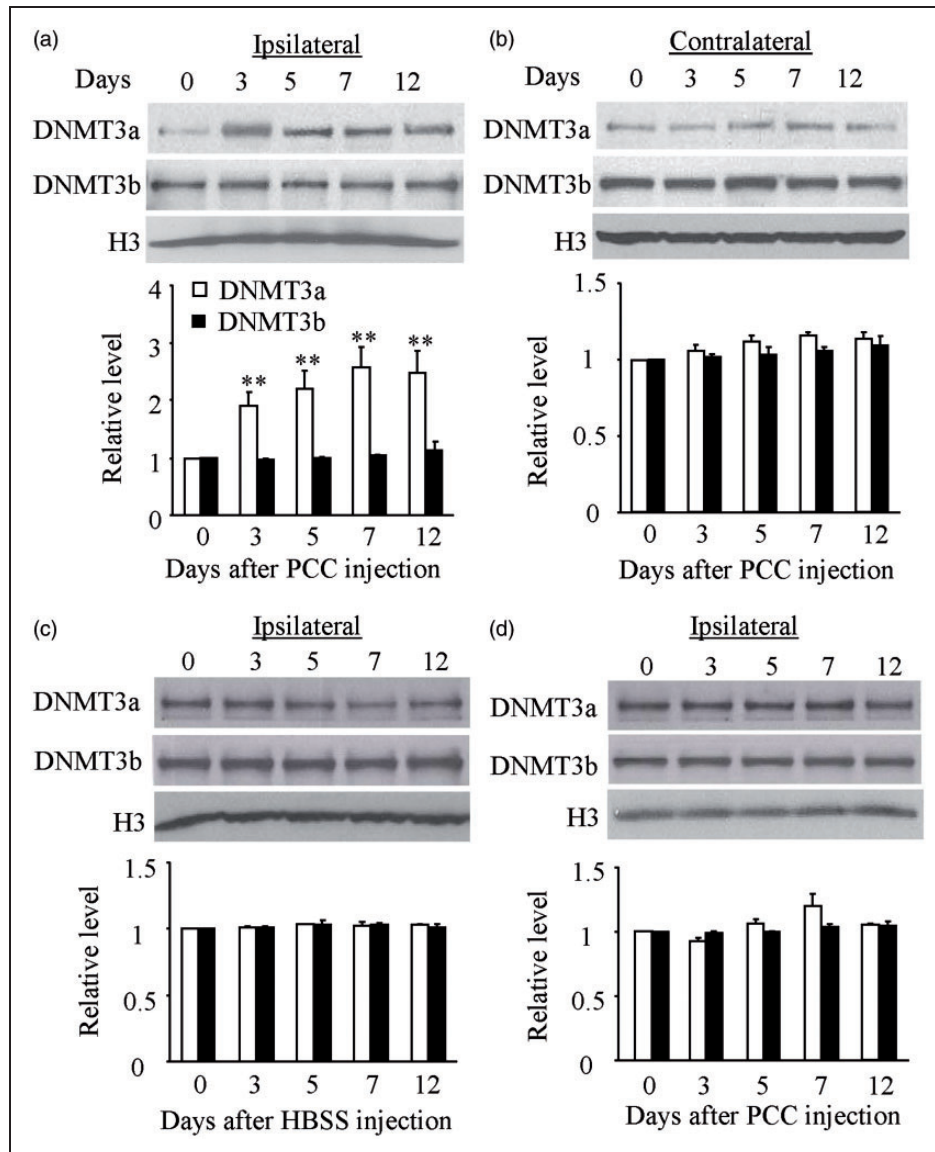


Figure 3. Time-dependent increase of DNMT3a in the ipsilateral L4/5 spinal dorsal horn, but not L4/5 DRG, after prostate cancer cell (PCC) injection. (a) The amounts of DNMT3a protein, but not DNMT3b protein, were significantly increased in the ipsilateral L4/5 dorsal horn on days 3, 5, 7, and 12 after PCC injection. $n = 3/\text{time point}$. One-way ANOVA followed by post hoc Tukey's test. $**P < 0.01$ versus the corresponding naive rats (0 day). (b) PCC injection did not lead to changes in basal expression of DNMT3a and DNMT3b in the contralateral L4/5 dorsal horn during the observation period. $n = 3/\text{time point}$. One-way ANOVA followed by post hoc Tukey's test. (c) Basal expression of both DNMT3a and DNMT3b in the ipsilateral L4/5 dorsal horn was not altered after Hank's balanced salt solution (HBSS) injection. $n = 3/\text{time point}$. One-way ANOVA followed by post hoc Tukey's test. (d) PCC injection did not lead to changes in basal expression of DNMT3a and DNMT3b in the ipsilateral L4/5 dorsal root ganglion during the observation period. $n = 3/\text{time point}$. One-way ANOVA followed by post hoc Tukey's test.

rats and on both ipsilateral and contralateral sides of HBSS-injected rats following dorsal horn microinjection of either virus (data not shown). These viral microinjected rats also displayed normal locomotor function including placing, grasping, and righting reflexes (Table 2).

Dorsal horn DNMT3a overexpression produces pain hypersensitivity

We further defined whether the early increase in dorsal horn DNMT3a was sufficient for bone cancer pain induction. AAV5-*Dnmt3a* or AAV5-GFP (as a control)

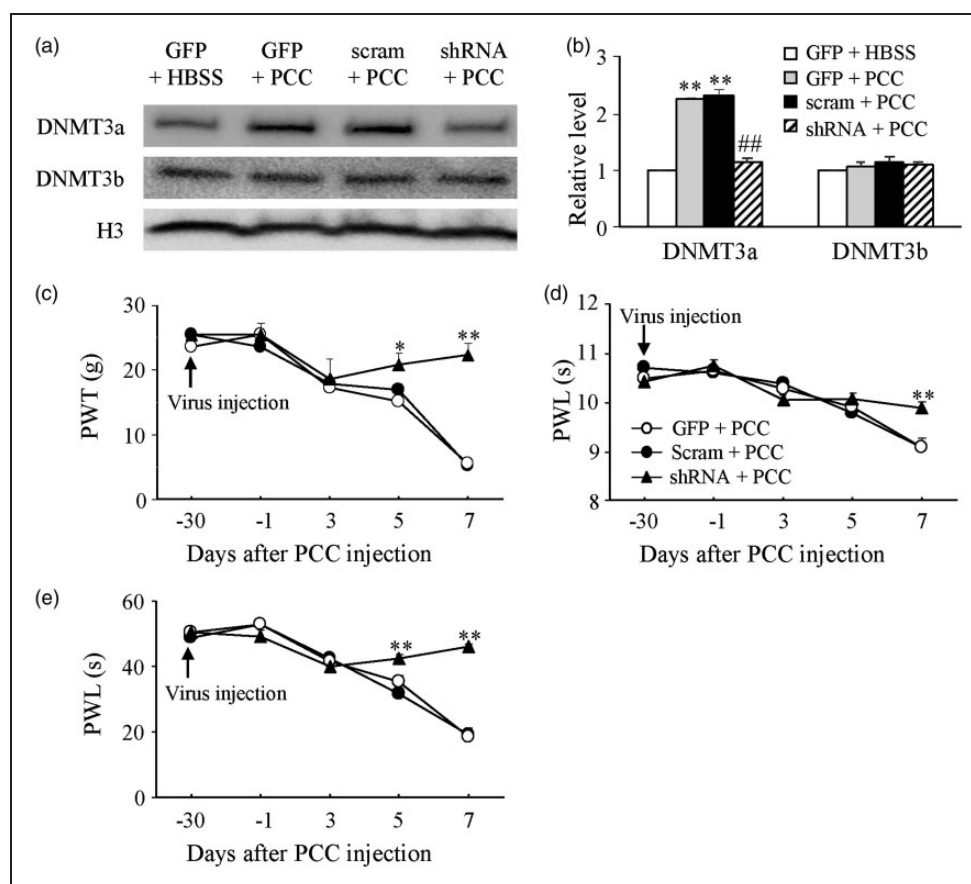


Figure 4. Effect of dorsal horn DNMT3a knockdown on the development of mechanical allodynia, thermal hyperalgesia, and cold allodynia induced by injecting prostate cancer cells (PCC) into the tibia. The level of DNMT3a, but not DNMT3b, increased in the ipsilateral L4/5 dorsal horn of rats microinjected with AAV5-GFP (GFP) or AAV5-*Dnmt3a* scrambled shRNA (Scram) on day 7 after PCC injection. This increase was abolished in the PCC rats microinjected with AAV5-*Dnmt3a* shRNA (shRNA). (a) Representative Western blots. (b) A summary of densitometric analysis. $n = 3/\text{group}$. One-way ANOVA followed by post hoc Tukey's test. $^{***}P < 0.01$ versus the corresponding AAV5-GFP plus HBSS group. $^{##}P < 0.01$ versus the corresponding AAV5-GFP plus PCC group. Microinjection of AAV5-*Dnmt3a* shRNA, but not AAV5-*Dnmt3a* scrambled shRNA and AAV5-GFP, into unilateral L4/5 dorsal horn 30 days before PCC injection blocked PCC-induced decreases in paw withdrawal threshold (PWT) to mechanical stimulation (c) and paw withdrawal latency (PWL) to thermal (d) and cold (e) stimuli on the ipsilateral side. $n = 5/\text{group}$. Two-way ANOVA followed by post hoc Tukey's test. $^{*}P < 0.05$, $^{**}P < 0.01$ versus the AAV5-GFP plus PCC group at the corresponding time points.

was microinjected into unilateral L4/5 dorsal horn of naive adult rats. Microinjection of AAV5-*Dnmt3a*, but not AAV-GFP, substantially increased the level of DNMT3a protein in dorsal horn, which occurred around 3–4 weeks and persisted for at least six weeks post-microinjection (Figure 5(a)). Microinjection of AAV5-*Dnmt3a* (not AAV5-GFP) led to mechanical allodynia, thermal hyperalgesia, and cold allodynia on the ipsilateral side, evidenced by significant and time-dependent decreases in paw withdrawal threshold to mechanical stimulation and paw withdrawal latencies to thermal and cold stimuli during the observation period (Figure 5(b) to (d)). Six weeks after viral microinjection, rats treated with AAV5-*Dnmt3a* ($n = 5$) exhibited decreases in paw withdrawal threshold to mechanical stimulation

by 70.9% ($P < 0.01$) and in paw withdrawal latencies to thermal and cold stimuli by 24.7% ($P < 0.01$) and 9.5% ($P < 0.01$), respectively, compared to the corresponding side of the AAV5-GFP-treated rats ($n = 5$, Figure 5(b) to (d)). Neither AAV5-*Dnmt3a* nor AAV5-GFP affected basal mechanical or thermal responses on the contralateral sides (Figure 5(b) to (d)) and locomotor function (Table 2) of the microinjected rats.

Contribution of DNMT3a to PCC-induced *Kvl.2* downregulation in spinal cord

Finally, we examined how the increased DNMT3a in spinal dorsal horn participated in bone cancer pain. Given that DNMT3a represses gene expression.^{9,12,14}

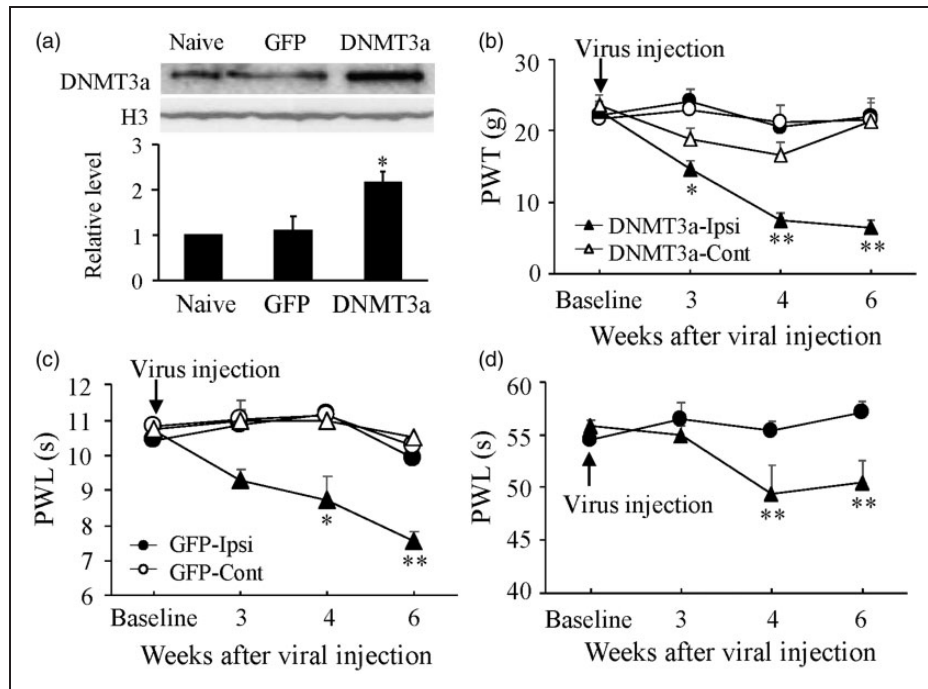


Figure 5. Dorsal horn DNMT3a overexpression led to mechanical allodynia, thermal hyperalgesia, and cold allodynia in naive rats. (a) The level of DNMT3a protein increased in the ipsilateral L4/5 dorsal horn 6 weeks after microinjection of AAV5-*Dnmt3a* (DNMT3a), but not AAV5-GFP (GFP), into unilateral L4/5 dorsal horn. Top: representative Western blots. Bottom: a summary of densitometric analysis. $n = 3/\text{group}$. One-way ANOVA followed by post hoc Tukey's test. $*P < 0.05$ versus naive rats. Microinjection of AAV5-*Dnmt3a*, but not AAV5-GFP, produced decreases in paw withdrawal threshold (PWT) to mechanical stimulation (b) and paw withdrawal latency to thermal (c) and cold (d) stimuli on the ipsilateral (Ipsi) side. Neither virus altered basal responses to mechanical (b) and thermal (c) stimuli on the contralateral (Cont) side. $n = 5/\text{group}$. Two-way ANOVA followed by post hoc Tukey's test. $*P < 0.05$, $**P < 0.01$ versus the AAV5-GFP group on the contralateral side at the corresponding time points.

we first examined whether the expression of some pain-related genes at the level of mRNA changed in the ipsilateral spinal dorsal horn after PCC injection. The level of *Kcna2* mRNA (encoding Kv1.2 protein) in the ipsilateral L4/5 dorsal horn on day 7 post-PCC (not HBSS) injection significantly decreased by 35% ($P < 0.01$) of the value of the naive group (Figure 6(a)). In contrast, neither PCC nor HBSS injection produced marked changes in the amounts of *Kcna1* mRNA, *Kcna4* mRNA, *Oprd1* mRNA, *Oprm1* mRNA, *Oprk1* mRNA, *Gad1* mRNA, and *Gad2* mRNA in the ipsilateral L4/5 dorsal horn on day 7 post-injection (Figure 6(a)). Furthermore, PCC injection led to a time-dependent reduction in Kv1.2 protein expression in the ipsilateral L4/5 dorsal horn (Figure 6(b)). The level of Kv1.2 on days 3, 5, 7, and 12 post-PCC injection was reduced by 1.2% ($P > 0.05$), 18.8% ($P > 0.05$), 33% ($P < 0.01$), and 16.9% ($P > 0.05$), respectively, as compared to naive rats (0d, Figure 6(b)). We found that this Kv1.2 reduction was related to the increased DNMT3a in dorsal horn after PCC injection, as demonstrated by the observation that blocking increased DNMT3a via microinjection of AAV5-*Dnmt3a* shRNA rescued the Kv1.2 expression in the L4/5 dorsal horn on day 7 post-PCC (Figure 6(c)).

Moreover, overexpression of DNMT3a via microinjection of AAV5-*Dnmt3a* reduced the level of Kv1.2 by 41% of the value in the naive group in L4/5 dorsal horn six weeks after microinjection ($P < 0.01$, Figure 6(d)). In addition, single cell RT-PCR analysis revealed co-expression of *Dnmt3a* mRNA with *Kcna2* mRNA in individual dorsal horn neurons (Figure 6(e)). Taken together, our data suggest that the increased DNMT3a triggers the Kv1.2 downregulation in dorsal horn neurons during PCC-induced bone cancer pain.

Discussion

The injection of PCC into tibia produced long-term mechanical allodynia, thermal hyperalgesia, and cold allodynia in a rat model, which mimics the clinical pain of patients with bone metastases. The present study demonstrated that the PCC-induced increase in dorsal horn DNMT3a is responsible for the downregulation of dorsal horn *Kcna2* mRNA and its encoding Kv1.2 protein as well as the development and maintenance of PCC-induced pain hypersensitivity. These findings suggest that DNMT3a contributes to bone cancer pain through epigenetic silencing of the *Kcna2* gene in

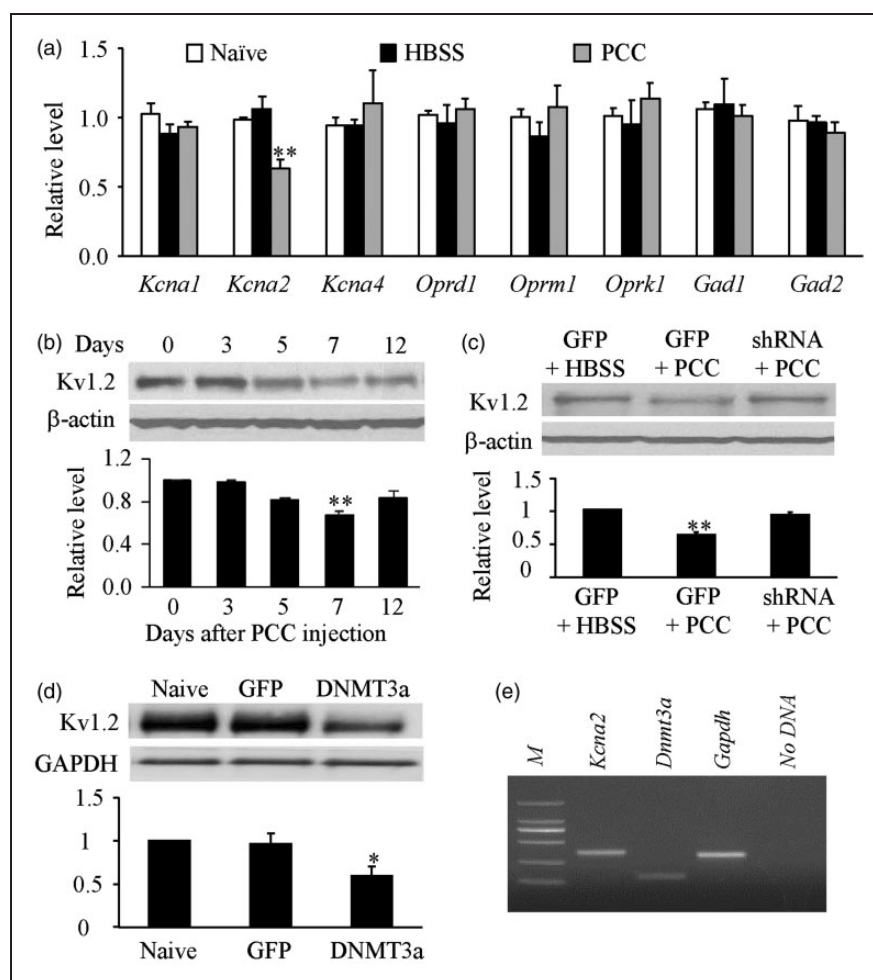


Figure 6. DNMT3a mediates PCC-induced Kv1.2 downregulation in dorsal horn. (a) The level of *Kcna2* mRNA, but not *Kcna1* mRNA, *Kcna4* mRNA, *Oprd1* mRNA, *Oprm1* mRNA, *Oprk1* mRNA, *Gad1* mRNA, and *Gad2* mRNA, decreased in the ipsilateral L4/5 dorsal horn on day 7 after PCC (not HBSS) injection. $n = 3/\text{group}$. One-way ANOVA followed by post hoc Tukey's test. $**P < 0.01$ versus naive rats. (b) Time-dependent reduction of Kv1.2 in the ipsilateral L4/5 dorsal horn post-PCC injection. Top: representative Western blots. Bottom: a summary of densitometric analysis. $n = 3/\text{time point}$. One-way ANOVA followed by post hoc Tukey's test. $**P < 0.01$ versus naive rats (0 day). (c) Microinjection of AAV5-*Dnmt3a* shRNA (shRNA), but not AAV5-GFP (GFP) and HBSS, rescued the expression of Kv1.2 in the ipsilateral L4/5 dorsal horn on day 7 post-PCC injection. Top: representative Western blots. Bottom: a summary of densitometric analysis. $n = 3/\text{time point}$. One-way ANOVA followed by post hoc Tukey's test. $**P < 0.01$ versus the AAV-GFP plus HBSS group. (d) Microinjection of AAV5-*Dnmt3a* (DNMT3a), but not AAV5-GFP (GFP), reduced the expression of Kv1.2 in the ipsilateral L4/5 dorsal horn 6 weeks after microinjection. Top: representative Western blots. Bottom: a summary of densitometric analysis. $n = 3/\text{time point}$. One-way ANOVA followed by post hoc Tukey's test. $*P < 0.05$ versus naive rats. (e) Co-expression of *Kcna2* mRNA with *Dnmt3a* mRNA in individual dorsal horn neurons from naive adult rats. *Gapdh* was used as a positive control. M: ladder marker. $n = 3$ repeats.

dorsal horn. DNMT3a may be a new potential target for cancer pain treatment.

DNMT3a protein is upregulated in a time-dependent manner in the ipsilateral L4/5 dorsal horn, but not in the contralateral L4/5 dorsal horn or bilateral L4/5 DRG after PCC injection into unilateral tibia. Interestingly, spinal nerve ligation-induced peripheral nerve injury upregulated DNMT3a expression in the ipsilateral DRG but not in the bilateral dorsal horn,^{15,17} whereas hind paw inflammation caused by injection of complete Freund's adjuvant did not change basal expression of

DNMT3a in the DRG and spinal cord on either ipsilateral or contralateral sides.¹⁷ DNMT3a upregulation appears to be tissue- and peripheral noxious stimulation specific. PCC-induced DNMT3a upregulation occurs likely in dorsal horn neurons, as DNMT3a protein was detected in mouse dorsal horn neurons.³³ Our single cell RT-PCR assay also showed the expression of *Dnmt3a* mRNA in rat individual dorsal horn neurons. To further rule out the possibility that the upregulated DNMT3a occurs in dorsal horn glial cells, the double labeling of DNMT3a with markers of dorsal horn astrocytes

(GFAP) and microglia (OX-42) will be carried out when the antibody against DNMT3a is available for immunostaining in the tissues of Copenhagen rats.

The increased DNMT3a may participate in PCC-induced downregulation of the *Kcna2* gene in ipsilateral dorsal horn. PCC injection downregulated the expression of *Kcna2* mRNA and its coding protein Kv1.2 in the ipsilateral dorsal horn on day 7 post-injection. This downregulation could be rescued by blocking the PCC-induced increase in dorsal horn DNMT3a through dorsal horn microinjection of AAV5-*Dnmt3a* shRNA. Moreover, mimicking the PCC-induced increase in dorsal horn DNMT3a via its genetic overexpression reduced the expression of Kv1.2 protein in the dorsal horn of naive rat. Given that *Dnmt3a* mRNA co-expresses with *Kcna2* mRNA in the individual dorsal horn neurons and that DNMT3a is a gene transcription repressor,^{9,12,14} it is likely that an elevation of DNA methylation within the *Kcna2* gene promoter caused by the increased DNMT3a interferes with the binding of transcription factors and/or serves as docking sites for methyl-CpG-binding domain proteins, resulting in *Kcna2* gene silencing in the dorsal horn neurons under CPP-induced bone cancer pain conditions, although the detailed mechanisms remain to be confirmed. It should be stated that *Kcna2* gene expression can be regulated through other epigenetic mechanisms. For example, G9a-triggered histone methylation and endogenous long non-coding *Kcna2* antisense RNA are involved in nerve injury-induced *Kcna2* silencing in the injured DRG.^{21,32} Whether these mechanisms also participate in PCC-induced downregulation of dorsal horn *Kcna2* gene are unclear and will be addressed in future studies.

The increased DNMT3a contributes to the development and maintenance of bone cancer pain partially through the silencing of Kv1.2 expression in dorsal horn. Kv1.2 is expressed widely in the neurons of nervous system including spinal cord and DRG and is a key player in establishing resting membrane potential and controlling neuronal excitability. Kv1.2 knockdown depolarizes the resting membrane potential, decreases the current threshold for action potential generation, and increases the number of action potentials in DRG neurons and produced neuropathic pain symptoms.^{17,21,32} In contrast, blocking the nerve injury-induced reduction of DRG Kv1.2 alleviated neuropathic pain.^{17,21,32} It is likely that PCC-induced dorsal horn Kv1.2 downregulation, like nerve injury-induced DRG Kv1.2 reduction, may also alter the electrophysiological characteristics of dorsal horn neurons, which produces dorsal horn neuronal hyperexcitability and results in pain hypersensitivity under PCC-induced bone cancer pain conditions. This conclusion is strongly supported by our observations that rescuing Kv1.2 expression by blocking increased DNMT3a in dorsal horn attenuated

PCC-induced bone cancer pain development and maintenance and that downregulating Kv1.2 expression through DNMT3a overexpression in dorsal horn led to pain hypersensitivity in naive rats. It is worth noting that dorsal horn Kv1.2 expression was significantly reduced only on day 7 post-PCC, at this time point PCC-induced pain hypersensitivity reaches a peak. The time course change of dorsal horn Kv1.2 expression did not parallel that of dorsal horn DNMT3a expression or PCC-induced behavioral responses post-PCC. DNMT3a appears to have other downstream targets that participate in bone cancer pain genesis. Indeed, some other potassium channels, such as A-type potassium channels, ATP-sensitive potassium channels, and Kv7, play a role in cancer pain development.^{34–38} Although we reported that PCC injection did not alter the expression of *Kcna1*, *Kcna4*, *Oprd1*, *Oprm1*, *Oprk1*, *Gad1*, and *Gad2* in dorsal horn, whether the DNMT3a-triggered changes in the expression of these potassium channels in dorsal horn post-PCC will be further examined.

In conclusion, the current study demonstrates a DNMT3a-triggered epigenetic mechanism of *Kcna2* downregulation in the dorsal horn under bone cancer pain conditions. Given that blocking increased dorsal horn DNMT3a impaired PCC-induced pain hypersensitivity during the development and maintenance periods without affecting acute pain and locomotor functions, DNMT3a is a possible target for cancer pain management. Yet, the potential side effects caused by systemic DNMT3a inhibition should be considered as it is expressed systemically.

Author contributions

YXT conceived the project and supervised all experiments. XRM, LCF, and YXT designed the project. XRM, LCF, SW, QXM, ZL, and JX performed molecular, biochemical, surgery, microinjection, and behavioral experiments. XRM, LCF, ZJL, and YXT analyzed the data. XRM and YXT wrote the manuscript. All of the authors read and discussed the manuscript.

Declaration of Conflicting Interests

The author(s) declared no potential conflicts of interest with respect to the research, authorship, and/or publication of this article.

Funding

The author(s) disclosed receipt of the following financial support for the research, authorship, and/or publication of this article: This work was supported by NIH grants (R01NS094664, R01NS094224, R01DA033390, and U01HL117684) to YXT and by the National Natural Science Foundation of China (81100276) to XRM.

References

1. Mantyh PW. Cancer pain and its impact on diagnosis, survival and quality of life. *Nat Rev Neurosci* 2006; 7: 797–809.
2. Bubendorf L, Schopfer A, Wagner U, et al. Metastatic patterns of prostate cancer: an autopsy study of 1,589 patients. *Hum Pathol* 2000; 31: 578–583.
3. Mercadante S. Malignant bone pain: pathophysiology and treatment. *Pain* 1997; 69: 1–18.
4. Gaskin DJ and Richard P. The economic costs of pain in the United States. *J Pain* 2012; 13: 715–724.
5. Clohisey DR and Mantyh PW. Bone cancer pain. *Cancer* 2003; 97: 866–873.
6. Schwei MJ, Honore P, Rogers SD, et al. Neurochemical and cellular reorganization of the spinal cord in a murine model of bone cancer pain. *J Neurosci* 1999; 19: 10886–10897.
7. Svendsen KB, Andersen S, Arnason S, et al. Breakthrough pain in malignant and non-malignant diseases: a review of prevalence, characteristics and mechanisms. *Eur J Pain* 2005; 9: 195–206.
8. Shih MH, Kao SC, Wang W, et al. Spinal cord NMDA receptor-mediated activation of mammalian target of rapamycin is required for the development and maintenance of bone cancer-induced pain hypersensitivities in rats. *J Pain* 2012; 13: 338–349.
9. Liang L, Lutz BM, Bekker A, et al. Epigenetic regulation of chronic pain. *Epigenomics* 2015; 7: 235–245.
10. Lutz BM, Bekker A and Tao YX. Noncoding RNAs: new players in chronic pain. *Anesthesiology* 2014; 121: 409–417.
11. Jeltsch A. Molecular enzymology of mammalian DNA methyltransferases. *Curr Top Microbiol Immunol* 2006; 301: 203–225.
12. Poetsch AR and Plass C. Transcriptional regulation by DNA methylation. *Cancer Treat Rev* 2011; 37(Suppl 1): S8–12.
13. Siedlecki P and Zielenkiewicz P. Mammalian DNA methyltransferases. *Acta Biochim Pol* 2006; 53: 245–256.
14. Turek-Plewa J and Jagodzinski PP. The role of mammalian DNA methyltransferases in the regulation of gene expression. *Cell Mol Biol Lett* 2005; 10: 631–647.
15. Sun L, Zhao JY, Gu X, et al. Nerve injury-induced epigenetic silencing of opioid receptors controlled by DNMT3a in primary afferent neurons. *Pain* 2017; 158: 1153–1165.
16. Wang Y, Liu C, Guo QL, et al. Intrathecal 5-azacytidine inhibits global DNA methylation and methyl-CpG-binding protein 2 expression and alleviates neuropathic pain in rats following chronic constriction injury. *Brain Res* 2011; 1418: 64–69.
17. Zhao JY, Liang L, Gu X, et al. DNA methyltransferase DNMT3a contributes to neuropathic pain by repressing Kcna2 in primary afferent neurons. *Nat Commun* 2017; 8: 14712.
18. Zhou XL, Yu LN, Wang Y, et al. Increased methylation of the MOR gene proximal promoter in primary sensory neurons plays a crucial role in the decreased analgesic effect of opioids in neuropathic pain. *Mol Pain* 2014; 10: 51.
19. Fan L, Guan X, Wang W, et al. Impaired neuropathic pain and preserved acute pain in rats overexpressing voltage-gated potassium channel subunit Kv1.2 in primary afferent neurons. *Mol Pain* 2014; 10: 8.
20. Li Z, Gu X, Sun L, et al. Dorsal root ganglion myeloid zinc finger protein 1 contributes to neuropathic pain after peripheral nerve trauma. *Pain* 2015; 156: 711–721.
21. Zhao X, Tang Z, Zhang H, et al. A long noncoding RNA contributes to neuropathic pain by silencing Kcna2 in primary afferent neurons. *Nat Neurosci* 2013; 16: 1024–1031.
22. Xu JT, Zhou X, Zhao X, et al. Opioid receptor-triggered spinal mTORC1 activation contributes to morphine tolerance and hyperalgesia. *J Clin Invest* 2014; 124: 592–603.
23. Xu JT, Sun L, Lutz BM, et al. Intrathecal rapamycin attenuates morphine-induced analgesic tolerance and hyperalgesia in rats with neuropathic pain. *Transl Perioper Pain Med* 2015; 2: 27–34.
24. Yaster M, Guan X, Petralia RS, et al. Effect of inhibition of spinal cord glutamate transporters on inflammatory pain induced by formalin and complete Freund's adjuvant. *Anesthesiology* 2011; 114: 412–423.
25. Zhang B, Tao F, Liaw WJ, et al. Effect of knock down of spinal cord PSD-93/chapsin-110 on persistent pain induced by complete Freund's adjuvant and peripheral nerve injury. *Pain* 2003; 106: 187–196.
26. Zhang J, Liang L, Miao X, et al. Contribution of the suppressor of Variegation 3-9 Homolog 1 in dorsal root ganglia and spinal cord dorsal horn to nerve injury-induced nociceptive hypersensitivity. *Anesthesiology* 2016; 125: 765–778.
27. Zhang RX, Liu B, Wang L, et al. Spinal glial activation in a new rat model of bone cancer pain produced by prostate cancer cell inoculation of the tibia. *Pain* 2005; 118: 125–136.
28. Li Z, Mao Y, Liang L, et al. The transcription factor C/EBPbeta in the dorsal root ganglion contributes to peripheral nerve trauma-induced nociceptive hypersensitivity. *Sci Signal* 2017; 10: eaam5345.
29. Liaw WJ, Zhang B, Tao F, et al. Knockdown of spinal cord postsynaptic density protein-95 prevents the development of morphine tolerance in rats. *Neuroscience* 2004; 123: 11–15.
30. Tao YX, Rumbaugh G, Wang GD, et al. Impaired NMDA receptor-mediated postsynaptic function and blunted NMDA receptor-dependent persistent pain in mice lacking postsynaptic density-93 protein. *J Neurosci* 2003; 23: 6703–6712.
31. Dixon WJ. Efficient analysis of experimental observations. *Annu Rev Pharmacol Toxicol* 1980; 20: 441–462.
32. Liang L, Gu X, Zhao JY, et al. G9a participates in nerve injury-induced Kcna2 downregulation in primary sensory neurons. *Sci Rep* 2016; 6: 37704.
33. Chestnut BA, Chang Q, Price A, et al. Epigenetic regulation of motor neuron cell death through DNA methylation. *J Neurosci* 2011; 31: 16619–16636.
34. Duan KZ, Xu Q, Zhang XM, et al. Targeting A-type K(+) channels in primary sensory neurons for bone cancer pain in a rat model. *Pain* 2012; 153: 562–574.
35. Xia H, Zhang D, Yang S, et al. Role of ATP-sensitive potassium channels in modulating nociception in rat model of bone cancer pain. *Brain Res* 2014; 1554: 29–35.

36. Zheng Q, Fang D, Liu M, et al. Suppression of KCNQ/M (Kv7) potassium channels in dorsal root ganglion neurons contributes to the development of bone cancer pain in a rat model. *Pain* 2013; 154: 434–448.
37. Cai J, Fang D, Liu XD, et al. Suppression of KCNQ/M (Kv7) potassium channels in the spinal cord contributes to the sensitization of dorsal horn WDR neurons and pain hypersensitivity in a rat model of bone cancer pain. *Oncol Rep* 2015; 33: 1540–1550.
38. Kanbara T, Nakamura A, Takasu K, et al. The contribution of Gi/o protein to opioid antinociception in an oxaliplatin-induced neuropathy rat model. *J Pharmacol Sci* 2014; 126: 264–273.